A00-33786

# AIAA 2000-2308

# Numerical and Theoretical Studies of the Instability of Low-Reynolds-Number Separation Bubbles

Mahidhar Tatineni and Xiaolin Zhong
University of California, Los Angeles
Los Angeles, CA

**Fluids 2000**
19-22 June , 2000 / Denver, CO

# NUMERICAL AND THEORETICAL STUDIES OF THE INSTABILITY OF LOW-REYNOLDS-NUMBER SEPARATION BUBBLES

Mahidhar Tatineni* and Xiaolin Zhong†
University of California, Los Angeles, California 90095

## Abstract

Low-Reynolds-number flows over airfoils are often characterized by the presence of separation bubbles, which can be unsteady with vortex shedding. The present study uses computational studies and linear stability theory to study the stability characteristics of incompressible low-Reynolds-number separation bubbles. A three dimensional time accurate numerical procedure is developed for simulations of transitional separation bubbles. The numerical method is fifth order accurate in the streamwise and wall normal direction and uses a spectral method in the spanwise direction. The numerical simulations are used to study flat plate separation bubble test cases. The separation bubbles on the flat plate are induced by specifying a velocity gradient in the freestream. The stability characteristics of the separated flow are studied by introducing controlled disturbances upstream of the separation bubble. A number of cases with different two dimensional initial disturbance amplitudes have been studied.

## INTRODUCTION

Low-Reynolds-number aerodynamics, in the range of $Re = 5 \times 10^4$ to $1 \times 10^6$, is important for a variety of aircrafts, ranging from sailplanes and human-powered aircrafts to high altitude unmanned aerial vehicles (UAV's) [1,2]. This research is motivated in part by its relevance to the APEX high-altitude aircraft research project at NASA Dryden [1]. The APEX project at NASA Dryden Flight Research Center plans to use the APEX high altitude aircraft to collect aerodynamic data for transonic low-Reynolds-number flows, with separation bubbles, over airfoils.

Early interest in low-Reynolds-number separation bubbles was motivated by performance studies of thin airfoil sections. The pressure distributions from the experimental studies revealed the presence of "short" and "long" separation bubbles on the airfoil surfaces [3-5]. The separation bubble is formed because the laminar boundary-layer over the airfoil separates due to the adverse pressure gradient. In some instances the separated boundary layer may reattach to form a shallow region of reverse flow, which is a laminar separation bubble. However, the early experiments [3-5] showed that under certain conditions the separated flow may not reattach, and subsequently become turbulent. The turbulent flow reattaches to form a "long" separation bubble. Gaster [6] experimentally studied laminar separation bubbles at a wide range of Reynolds numbers and angle of attacks and studied the conditions under which bursting occurs. The instability of the separated flow, and the subsequent transition to turbulence, has been studied experimentally by Blackwelder et. al. [7] and Dovgal et. al. [8]. Blackwelder et. al. [7] showed that the dominant frequency in the flowfield matches with the most unstable frequency predicted by linear stability theory. Dovgal et. al. [8] showed the presence of feedback effects, and found that introducing disturbances of amplitudes above a certain critical level resulted in a change in the overall time-averaged mean flow.

Theoretical studies of separation bubbles are based on the triple deck theory or on the interactive boundary layer theory. These theories are required because the traditional boundary layer theory fails at the separation location due to a singularity in the boundary layer solution [9]. Stewartson, Smith and Kaups [10] developed a theory for marginal separation problems based on the triple deck theory to avoid this singularity. This approach can be used for problems with relatively weak pressure gradients and is valid for $Re \rightarrow \infty$. This method has been applied to study qausi-two-dimensional [11] and unsteady three-dimensional [12] boundary layer flow. A quantitative study of the accuracy of the triple deck solution at finite Reynolds-numbers was done by Hsiao and Pauley [13]. They showed that the Reynolds-number based on the pressure gradient length gives an appropriate criteria to describe the accuracy of the triple deck method. In addition, Hsiao and Pauley [13] also showed that the interactive boundary layer method is the most efficient method for solving a flow with small separation bubbles. Hence, for a sufficiently gradual adverse pressure gradient the triple deck method and the interactive boundary layer method can be used to solve the problem. However, when the pressure gradient is increased the marginal separation formulation begins to fail. This led to the

*Graduate Student, Member AIAA.
†Associate Professor, Mechanical and Aerospace Engineering Department, Senior Member AIAA, xiaolin@seas.ucla.edu.

development of an unsteady nonlinear triple-deck system by Vickers and Smith [14]. In their formulation additional equations are developed to resolve the detached shear layer far beyond the separation point. When combined with the triple deck formulation for the breakaway separation it enables a theoretical study of the unsteady separation and the inflexional modes associated with the detached shear layer. This formulation is a good tool to analyze the transitional separation bubbles.

Early numerical studies of separation bubbles relied on 2-D steady Navier-Stokes or boundary layer calculations coupled with transition models [15–18]. These studies were an efficient tool for predicting aerodynamic performance of airfoils in the low-Reynolds-number regime. However, the 2-D incompressible simulations of Lin and Pauley [19] showed the unsteady nature of the separation bubbles, and the vortex shedding associated with the instability of the separated flows. Their results showed that it was important to capture the unsteady nature of the flowfield. Our previous incompressible and compressible 2-D simulations [20,21] of flow over the APEX airfoil showed the same vortex shedding process. An analysis of the numerical results showed that the growth of disturbance waves in the separated region leads to the vortex shedding. The dominant frequency from the numerical simulations is found to agree with the most unstable frequency from a linear stability analysis. Three dimensional effects in separation bubbles for flows over a flat plate have been studied by Hildings [22] and Rist and Maucher [23]. Rist and Maucher introduced various two-dimensional and three-dimensional disturbances into the flowfield to study the nonlinear disturbance development in the separation bubble. Their simulations were able to obtain a turbulent flowfield and predicted longitudinal vortices in the reattachment region. Alam and Sandham [24] used direct numerical simulations of "short" laminar separation bubbles to show that the separated shear layer undergoes transition via oblique modes and vortex induced breakdown. Spalart and Strelets [25] numerically studied the transition process to show that the mechanism involves the instability of the shear layer producing Kelvin-Helmholtz vortices which breakdown. Recently, there has been some research on the control of two-dimensional unsteady separated flows. Zhang and Fasel evaluated the feasibility of flow control, by blowing and suction ahead of the separation bubble [26].

The extensive studies detailed above have shown the complex nature of the transitional separation bubbles. The numerical and experimental results have shown that the separation bubbles are very sensitive to freestream disturbances. Hence, there is a need to study the receptivity process in the separation bubbles. The stability analysis of inflexional velocity profiles has shown that the flow can be absolutely unstable under certain conditions. A detailed numerical study, supported by theoretical analysis, will be useful in this area. Experimental evidence has shown the presence of feedback effects. Numerical simulations can provide a controlled environment to study such effects. The objective of this paper is to analyze the stability of the separation bubbles using : (1) numerical simulations of separation bubbles, and (2) linear stability analysis of the separation bubbles. The numerical method is fifth order accurate in the streamwise and wall normal direction and uses a spectral method in the spanwise direction. The stability of the separated boundary layer is analyzed using a linear stability theory analysis assuming local parallel flow. The growth of disturbances in the separation bubbles is studied in greater detail by considering a flat plate separation test case. A separation bubble is formed by specifying a velocity gradient in the freestream. The growth of disturbances in the separation bubble is studied numerically.

## NUMERICAL METHODS

### 3-D Incompressible Navier-Stokes Solver

The numerical simulations are carried out using a fifth order 3-D incompressible solver. The formulation is based on the approach of Zhang and Fasel. [26] The governing equations for this test case are the incompressible Navier-Stokes equations in the vorticity transport form:

$$\frac{\partial \omega_x}{\partial t} + \frac{\partial}{\partial y}(v\omega_x - u\omega_y) - \frac{\partial}{\partial z}(u\omega_z - w\omega_x) = \Delta\omega_x \quad (1)$$

$$\frac{\partial \omega_y}{\partial t} - \frac{\partial}{\partial x}(v\omega_x - u\omega_y) + \frac{\partial}{\partial z}(w\omega_y - v\omega_z) = \Delta\omega_y \quad (2)$$

$$\frac{\partial \omega_z}{\partial t} + \frac{\partial}{\partial y}(u\omega_z - w\omega_x) - \frac{\partial}{\partial z}(w\omega_y - v\omega_z) = \Delta\omega_z \quad (3)$$

where

$$\Delta = \frac{1}{Re}\frac{\partial^2}{\partial x^2} + \frac{\partial^2}{\partial y^2} + \frac{1}{Re}\frac{\partial^2}{\partial z^2} \quad (4)$$

and the nondimensionalization is as follows:

$$x = \frac{x^*}{L}\ ,\ y = \sqrt{Re}\frac{y^*}{L}\ ,\ z = \frac{z^*}{L}\ , \quad (5)$$

$$u = \frac{u^*}{U_\infty}\ ,\ v = \sqrt{Re}\frac{v^*}{U_\infty}\ ,\ w = \frac{w^*}{U_\infty} \quad (6)$$

where the $*$'s represent the dimensional variables and $Re = U_\infty L/\nu$. The velocity components can be calculated from the following equations:

$$\frac{\partial^2 u}{\partial x^2} + \frac{\partial^2 u}{\partial z^2} = -\frac{\partial \omega_y}{\partial z} - \frac{\partial^2 v}{\partial x \partial y} \quad (7)$$

$$\Delta v = \frac{\partial \omega_x}{\partial z} - \frac{\partial \omega_z}{\partial x} \quad (8)$$

$$\frac{\partial^2 w}{\partial x^2} + \frac{\partial^2 w}{\partial z^2} = \frac{\partial \omega_y}{\partial x} - \frac{\partial^2 v}{\partial y \partial z} \quad (9)$$

The Blasius boundary layer solution is prescribed at the inlet. No slip conditions are used on the wall, except in the disturbance strip region where the normal velocity is specified. At the freestream, the streamwise velocity is specified and the vorticity is set to zero. The equations are solved using an explicit fourth order Runge-Kutta scheme in time coupled with fifth order upwind finite differencing in the streamwise and wall-normal directions, and a pseudospectral fourier method in the spanwise direction. The separation bubble is generated by prescribing a deceleration in the freestream velocity. Controlled disturbances can be introduced in the flowfield by blowing and suction at the wall upstream of the separation bubble as illustrated in the schematic in Fig. 1 (b). The disturbance form is as follows:

$$V_k(x,0,t) = A_k\sqrt{Re}v_w(x)sin(\beta t) \qquad (10)$$

where $v_w(x)$ is the wall-forcing function, $k$ is the fourier mode number (in the z direction) and $\beta$ is the nondimensional frequency. $v_w(x)$ is zero everywhere except within the disturbance strip, where a point-symmetric amplitude distribution with respect to the center of the strip is used. Upstream of the outflow boundary, the disturbances are forced to decay using a fringe region. The fringe operates by gradually suppressing the disturbance vorticity [23]. The separation and transition processes will be studied by considering a number of 2-D and 3-D disturbances. The disturbances amplitudes and frequencies will be changed to obtain linear and nonlinear effects.

### Linear Stability Analysis

The stability characteristics of the separated flow are analyzed using linear stability theory. The governing Navier-Stokes equations are linearized and the following disturbance form is assumed:

$$q(y) = \tilde{q}(y)e^{(\alpha x+\beta z-i\omega t)} \qquad (11)$$

where $q = (u', v', p')$, and $\tilde{q}$ are the corresponding eigenfunctions obtained from a linear stability analysis. The locally parallel flow assumption is made in the analysis. The equations are discretized using a fourth order finite difference method, and the resulting eigenvalue problem is solved. In this paper a spatial analysis is performed, i.e. $\omega$ and $\beta$ are specified and $\alpha$ is calculated as the eigenvalue.

## RESULTS

The incompressible code was validated using a flat plate boundary layer test case. The validated solver was then used to compute a flat plate separation bubble test case. The separation bubble is induced by specifying a velocity gradient in the freestream. A steady separation bubble is obtained. The unsteady characteristics are studied by introducing disturbances upstream of the separation bubble. The details of the numerical results are presented below.

### Flat Plate Boundary Layer Validation Case

The fifth order incompressible explicit Navier-Stokes code was used to compute a flat plate boundary layer test case. The flow variables are nondimensionalized as follows:

$$x = \frac{x^*}{L}\ ,\ y = \sqrt{Re}\frac{y^*}{L}\ ,\ z = \frac{z^*}{L}\ ,$$
$$u = \frac{u^*}{U_\infty}\ ,\ v = \sqrt{Re}\frac{v^*}{U_\infty}\ ,\ w = \frac{w^*}{U_\infty} \qquad (12)$$

In this test case the Reynolds number $Re$=$10^5$ and the characteristic length $L$=$0.05m$. The domain ranges $x_o = 0.37(Re_\delta$=$331)$ to $x_N = 2.06(Re_\delta$=$781)$ in the x-direction and the maximum in the wall normal direction is $y_N = 18.84(= 18\delta_o)$. The disturbance test case chosen was a 2-D disturbance induced by blowing and suction upstream of the flow. The disturbance is induced at a blowing and suction strip from $x = 0.55$ to $x = 0.70$. The disturbance form is as follows:

$$V(x,0,t) = A\sqrt{Re}v_w(x)sin(\beta t)$$

where $v_w(x)$ is the wall-forcing function, and $\beta$ is the nondimensional frequency. $v_w(x)$ is zero everywhere except within the disturbance strip, where a point-symmetric fifth order polynomial amplitude distribution with respect to the center of the strip is used. The disturbance is purely 2-dimensional, the amplitude A is $10^{-6}$, and $\beta = 10.8(F = \frac{\beta^*\nu^*}{U_\infty^2}10^4 = 1.08)$. The disturbance is allowed to grow spatially through the domain and the results compared with linear stability theory. Figure 2 shows the instantaneous disturbance vorticity contours. Near the end of the domain the contours disappear since the fringe damps the disturbances out. Figure 3 shows the comparison of the disturbance streamwise velocity eigenfunction with the linear stability results at $x = 1.05$. Both the real and imaginary parts are found to agree reasonably well with the linear stability results. There is a slight discrepancy near the freestream region because the boundary conditions in the simulations are different from the linear stability boundary conditions.

### Separation Bubble Case : Mean Flow

The validated fifth-order explicit Navier-Stokes code was used to compute a flat plate separation bubble test case similar to the case of Rist and Maucher [23]. The separation bubble is created by specifying a jump in the streamwise freestream velocity. The flow variables are

nondimensionalized as follows:

$$x = \frac{x^*}{L}\ ,\ y = \sqrt{Re}\frac{y^*}{L}\ ,\ z = \frac{z^*}{L}\ ,$$
$$u = \frac{u^*}{U_\infty}\ ,\ v = \sqrt{Re}\frac{v^*}{U_\infty}\ ,\ w = \frac{w^*}{U_\infty} \qquad (13)$$

In this test case the Reynolds number $Re = 10^5$ and the characteristic length $L$=0.05$m$. The domain ranges $x_o = 0.37(Re_\delta$=331) to $x_N = 5.06(Re_\delta$=1224) in the x-direction and the maximum in the wall normal direction is $y_N = 18.84(= 18\delta_o)$. The freestream velocity jump is prescribed using a fifth order polynomial from $x = 0.71$ to $x = 2.43$. The equation for the freestream velocity is as follows:

$x < 0.71$ :

$$u = 1; \qquad (14)$$

$0.71 < x < 2.43$ :

$$u = (1 - (1 + x_1 * 15/8) * \Delta u * 0.5), \qquad (15)$$
$$x_1 = (1/5 * x_2^5 - 2/3 * x_2^3 + x_2), \qquad (16)$$
$$x_2 = (2 * x - 3.14)/1.72 \qquad (17)$$

$x > 2.43$ :

$$u = 1 - \Delta u \qquad (18)$$

The 301 × 101 grid used in the simulations is shown in Fig. 4. Two test cases with velocity jumps of 8.8% and 9% are considered to study the sensitivity of the size of the separation bubble to the freestream pressure gradient. Figure 5 shows the separation streamline for both the cases, and the figure shows that the size of the bubble in the 9% velocity drop case is almost twice that in the 8.8% case. Hence, the size of the bubble is highly sensitive to the freestream pressure gradient. Figure 6 shows the streamwise velocity contours of the converged solution for both the cases. The corresponding vorticity distributions on the wall are shown in Fig. 7. The separation and reattachment points correspond to the zero vorticity locations. In both the cases the separation is steady, and can be classified as marginal separation. The velocity profiles are inflexional inside the bubble, and hence can be expected to be unstable. This is verified through a linear stability analysis below.

### Linear Stability Theory Results

The stability of the mean flow obtained from the numerical simulations is analyzed using a linear stability analysis. The disturbance form is as follows:

$$q(y) = \tilde{q}(y)e^{(\alpha x + \beta z - i\omega t)} \qquad (19)$$

where $q = (u', v', p')$, and $\tilde{q}$ are the corresponding eigenfunctions obtained from a linear stability analysis. The locally parallel flow assumption is made in the analysis. The linear stability analysis is carried out for $\beta = 0$, $\omega = 5.4, 18(F = \frac{\omega^* \nu^*}{U_\infty^2}10^4 = 0.54, 1.8)$ cases. Upstream of the separation bubble the dominant modes are the T-S waves. In the current cases the boundary layer is stable in the upstream region. However, in the separated region the flow is highly unstable since the velocity profiles are inflexional. Figure 8 shows the variation of the disturbance wavelengths in the separated region for the 9% velocity jump case. Figure 9 shows the growth rates in the separation region for the 9% velocity jump case. The results show a jump in the growth rates in the separation region, with the $\omega = 18$ case having the greater growth rates. It should be noted that the boundary layer without separation is stable in this region. Hence, the separation bubble is the cause of the highly unstable nature of the flowfield. Figure 10 compares the growth rates for the two velocity jump cases. The results clearly show that the 9% jump case is more unstable. Hence, the linear stability results predict instabilities in the separated region. These instabilities are also studied using numerical simulations as described below.

### Separation Bubble Case: Unsteady Results

The effect of disturbances on the separation bubble is evaluated by prescribing a wall normal velocity within a disturbance strip upstream of the separation bubble. The disturbance form is as follows:

$$V(x, 0, t) = A\sqrt{Re}v_w(x)sin(\beta t)$$

where $v_w(x)$ is the wall-forcing function, and $\beta$ is the nondimensional frequency. Fig. 11 shows the shape of the blowing and suction profile. The 9% velocity jump case is considered for two cases : (1) $\beta = 18(F = \frac{\beta^* \nu^*}{U_\infty^2}10^4 = 1.8)$, $A = 1 \times 10^{-6}$ and (2) $\beta = 5.4(F = \frac{\beta^* \nu^*}{U_\infty^2}10^4 = 0.54)$, $A = 1 \times 10^{-5}$. Figure 12 (a) shows the streamwise growth of disturbance wall normal velocity at $yRe^{0.5}/L = 0.36$ for case (1). The disturbance wall normal velocity contours for the same case are show in Fig. 12 (b). The growth of the disturbances in the separated region is clearly seen. At the end of the domain the fringe damps out the disturbances. The streamwise velocity eigenfunctions at various streamwise locations are plotted in Fig. 13. The first eigenfunction is in the region upstream of the separation bubble. Hence, the eigenfunction resembles eigenfunctions associated with first mode T-S waves. However, within the separated region (next three eigenfunctions) the triple peak eigenfunctions are seen. The triple peak eigenfunction seen at $i = 100$ is similar to results from experimental observations of Dovgal et. al. [8]. Beyond the separation bubble region the eigenfunctions return to the first-mode shapes. Figure 14 shows the streamwise growth of disturbance wall normal velocity at $yRe^{0.5}/L = 0.36$ for case (2). The disturbance wall normal velocity con-

tours for the same case are show in Fig. 15. In this case the growth continues beyond the separation region. This is possibly due to the presence of nonlinear effects. However, further computations are required to ascertain nonlinear effects, and to study the transition process.

## SUMMARY

A framework for studying the stability of laminar separation bubbles has been developed. The size of the steady separation bubble is found to be very sensitive to the freestream pressure gradient imposed. The unsteady two-dimensional numerical results obtained so far have shown that the separation bubbles are highly unstable and greatly amplify disturbances. The amplification of the disturbances in the separated region leads to unsteady vortex shedding. This unstable nature of the separated flow has been verified through a linear stability analysis. Future work will be focused on three dimensional simulations to study the transition process in detail. In addition, a theoretical approach based on triple deck theory will also be used to supplement the numerical simulations.

### Acknowledgments

This research has been supported by NASA Dryden Flight Research Center under Grant NCC 2-374.

### References

[1] Murray, J., Moes, T., K.Norlin, J.Bauer, Geenen, R., Moulton, B., and Hoang., S., "Piloted simulation study of a balloon-assisted deployment of an aircraft at high altitude." *NASA-TM 104245*, 1992.

[2] Lissman, P., "Low Reynolds number airfoils." *Annual Review of Fluid Mechanics*, 1983, pp. 223–239.

[3] Owen, P. and Klanfer., L., *ARC 16*, 1953.

[4] McGregor, I., "Regions of Localised Boundary Layer Separation and Their Role in the Nose-Stalling of Aerofoils." *Ph.D. Thesis, Queens Mary College, University of London*, 1954.

[5] Crabtree, L., "The Formation of Regions of Separated Flow on Wing Surfaces." *ARC, R and M 3122*, 1959.

[6] Gaster, M., "The Structure and Behaviour of Laminar Separation Bubbles." *AGARD-CP-4*, Vol. 2, 1966, pp. 813–854.

[7] LeBlanc, P., Blackwelder, R., and Liebeck, R., "A Comparison Between Boundary Layer Measurements in a Laminar Separation Bubble Flow and Linear Stability Theory Calculations," *Perspectives in Turbulence Studies*, 1987, pp. 189–205.

[8] Dovgal, A., Kozlov, V., and Michalke, A., "Laminar Boundary Layer Separation: Instability and Associated Phenomena," *Progress in Aerospace Sciences*, Vol. 30, 1994, pp. 61–94.

[9] Goldstein, S., "On laminar boundary-layer flow near a separation point." *Quarterly Journal of Mech. Appl. Math*, Vol. 1, 1948, pp. 43–69.

[10] Stewartson, K., Smith, F., and Kaups, K., "Marginal Separation," *Studies in Applied Mathematics*, Vol. 67, 1982, pp. 45–61.

[11] Brown, S., "Marginal Separation of a Three Dimensional Boundary Layer on a Line of Symmetry," *Journal of Fluid Mechanics*, Vol. 159, 1985, pp. 95–111.

[12] Duck, P., "Three Dimensional Marginal Separation." *Journal of Fluid Mechanics*, Vol. 202, 1989, pp. 559–575.

[13] Hsiao, C. and Pauley, L., "The accuracy of the triple-deck theory for marginal separation," *FED-Vol.149, Separated Flows, ASME*, 1993.

[14] Vickers, I. and F.T.Smith, "Theory and computations for breakup of unsteady subsonic or supersonic separating flows," *Journal of Fluid Mechanics*, Vol. 268, 1994, pp. 147–173.

[15] Drela, M. and Giles., M., "Viscous-Inviscid analysis of transonic and low Reynolds number airfoils," *AIAA Journal*, Vol. 25(10), 1987, pp. 1347–1355.

[16] Schneider, J. and Ewald., B., *Integration of linear stability methods into Navier-Stokes solvers for computation of transonic laminar airfoils*, AIAA Paper 94-1849-CP, 1994.

[17] Vatsa, V. and Carter, J., "Analysis of Airfoil Leading-Edge Separation Bubbles," *AIAA Journal*, Vol. 22(12), 1984, pp. 1697–1704.

[18] Drela, M., "Transonic Low-Reynolds Number Airfoils," *Journal of Aircraft*, Vol. 29(6), 1992, pp. 1106–1113.

[19] Lin, J. M. and Pauley, L. L., "Low-Reynolds-Number Separation on an Airfoil," *AIAA Journal*, Vol. 34(8), 1996, pp. 1570–1577.

[20] Tatineni, M. and Zhong, X., "Numerical Simulation of Unsteady Low-Reynolds-Number Separated Flows Over Airfoils," *AIAA Paper 97-1929*, 1997.

[21] Tatineni, M. and Zhong, X., "Numerical Simulations of Unsteady Low-Reynolds-Number Separated Flows Over the APEX Airfoil," *AIAA Paper 98-0412*, 1998.

[22] Hildings, C., "Simulation of Laminar and Transitional Separation Bubbles," *Technical Reports from Royal Institute of Technology, Sweden*, Vol. Technical Report 1997:19, 1997.

[23] Rist, U. and Maucher, U., "Direct Numerical Simulation of 2-D and 3-D Instability Waves in a Laminar Separation Bubble," *AGARD-CP-551*, 1994.

[24] Alam, M. and Sandham, N. D., "Direct Numerical simulation of short laminar separation bubbles with turbulent reattachment," *Journal of Fluid Mechanics*, Vol. 403, 2000, pp. 223–250.

[25] Spalart, P. and Strelets, M. K., "Mechanisms of transition and heat transfer in a separation bubble," *Journal of Fluid Mechanics*, Vol. 403, 2000, pp. 329–349.

[26] Zhang, H. and Fasel, H., "Numerical Investigation of The Evolution and Control of Two-Dimensional Unsteady Separated Flow Over a Stratford Ramp," *AIAA Paper 99-1003*, 1999.

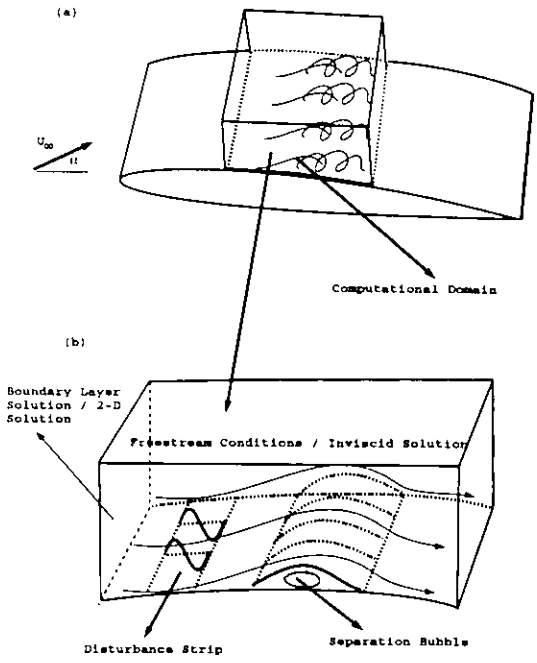


Figure 1: A schematic of the computational domain to be used for the localized direct numerical simulations (DNS) of the separation bubbles.

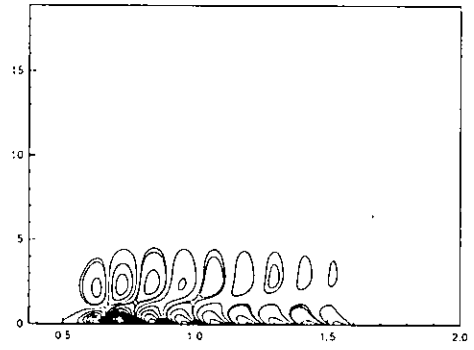


Figure 2: Instantaneous disturbance vorticity contours obtained from the numerical solutions for the flat plate boundary layer test case. The inlet Reynolds-number based on the distance from leading edge, ($Re_x = \frac{U_\infty x}{\nu}$) is $1 \times 10^5$.

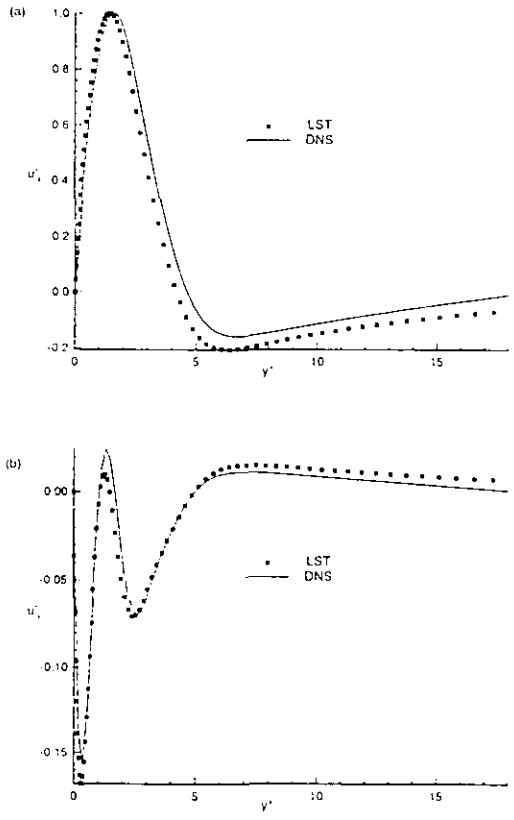


Figure 3: Comparison of numerical simulation and linear stability results for an instantaneous disturbance-u eigenfunction. Part (a) shows the real part and (b) shows the imaginary part. The inlet Reynolds-number based on the distance from leading edge, ($Re_x = \frac{U_\infty x}{\nu}$) is $1 \times 10^5$.

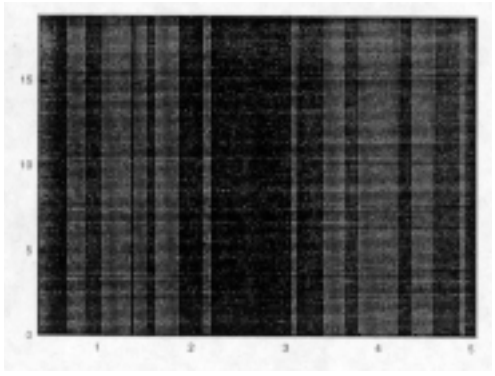

Figure 4: The 301 × 101 grid used for the mean flow computations of the separation bubble test case.

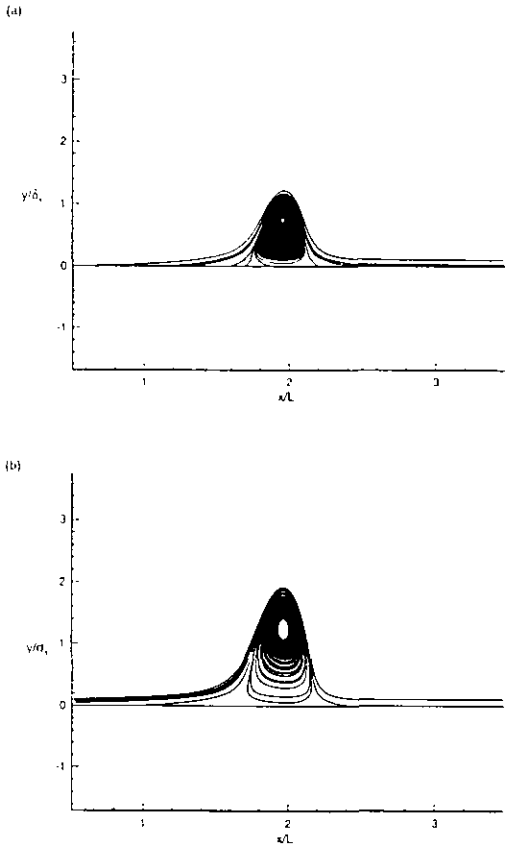


Figure 5: Mean flow separation streamlines for : (a) 8.8% freestream velocity drop (b) 9% freestream velocity drop .

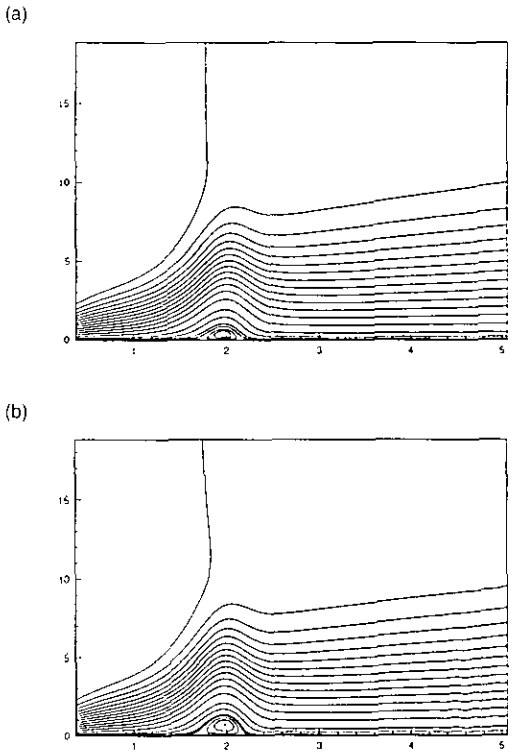


Figure 6: Mean flow velocity contours for the flat plate separation bubble test cases: (a) 8.8% freestream velocity drop (b) 9% freestream velocity drop .

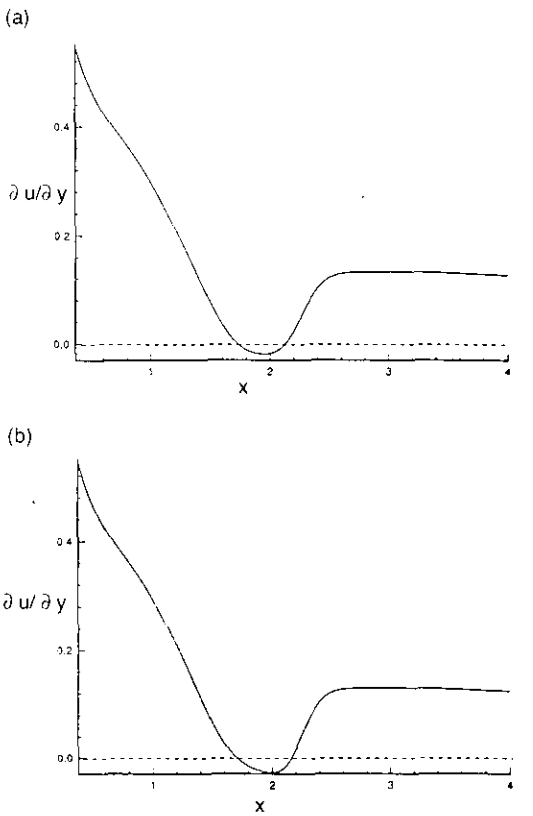


Figure 7: Wall vorticity variation for the flat plate separation bubble test cases:(a) 8.8% freestream velocity drop (b) 9% freestream velocity drop .

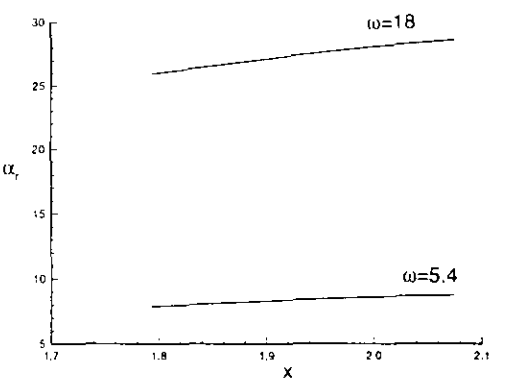


Figure 8: Disturbance wavelengths obtained from linear stability analysis and mean flow from numerical simulations. The separation bubble is induced by prescribing a 9% drop in the freestream velocity.

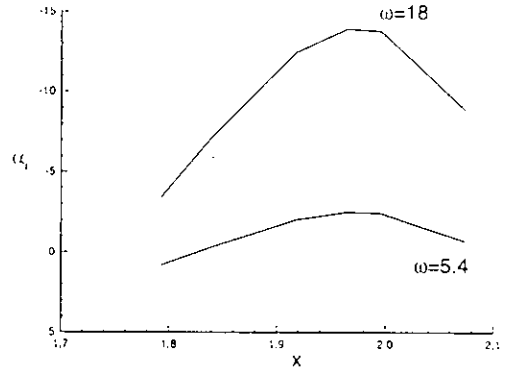


Figure 9: Disturbance growth rates obtained from linear stability analysis and mean flow from numerical simulations. The separation bubble is induced by prescribing a 9% drop in the freestream velocity.

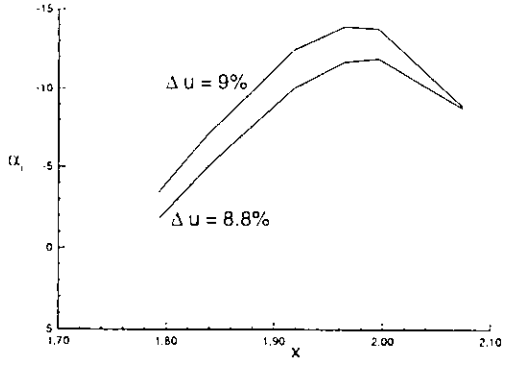


Figure 10: Comparison of disturbance growth rates, obtained from linear stability analysis, for the two separation bubble cases.

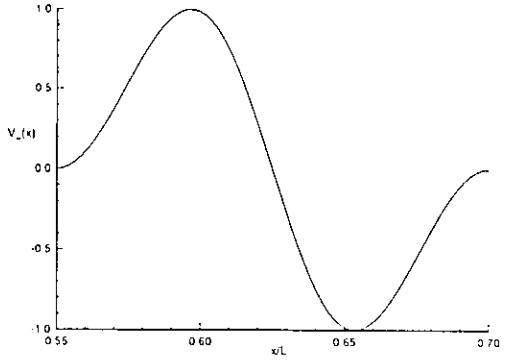


Figure 11: The blowing and suction profile used to induce disturbances for the flat plate separation bubble test case. The Reynolds number is $10^5$ and the reference length $L = 0.05m$.

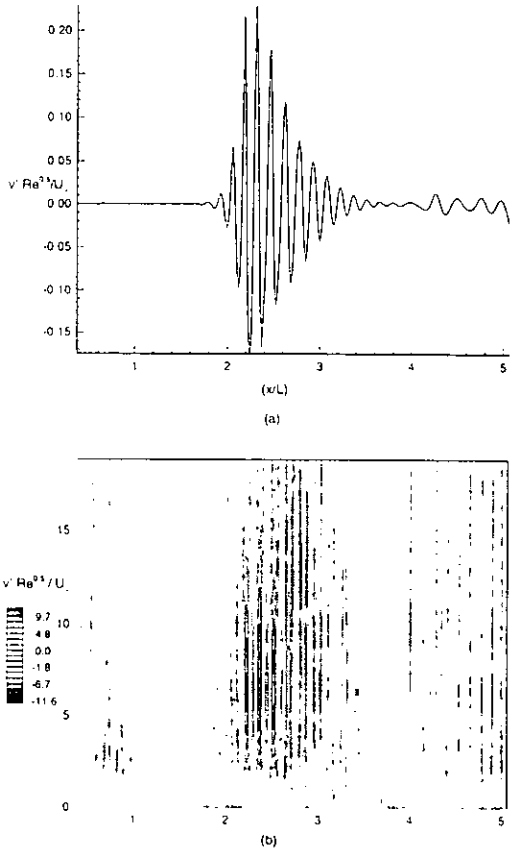


Figure 12: (a)The growth of disturbance wall normal velocity at $yRe^{0.5}/L = 0.36$, (b)disturbance wall normal velocity contours, for the flat plate separation bubble test case. The Reynolds-number is $10^5$ and the reference length $L = 0.05m$. The disturbances are introduced by blowing and suction at the wall upstream of the separation bubble. The mean flow is from the 9% velocity jump case.

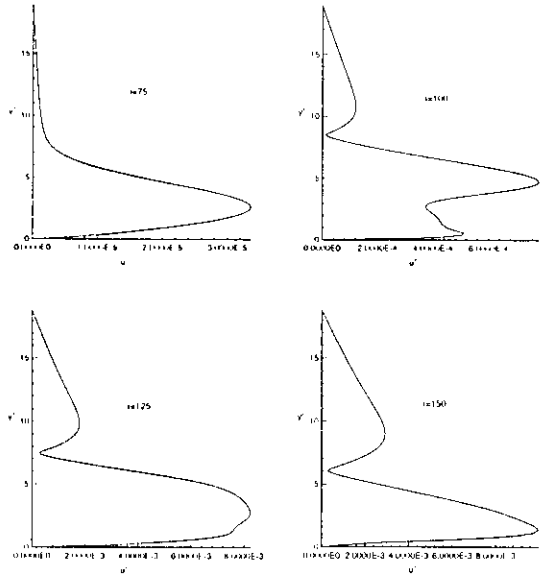

Figure 13: Streamwise disturbance velocity eigenfunction variations at different streamwise locations for the flat plate separation bubble test case. The Reynolds-number is $10^5$ and the reference length $L = 0.05m$. The disturbances are introduced by blowing and suction at the wall upstream of the separation bubble. The mean flow is from the 9% velocity jump case.

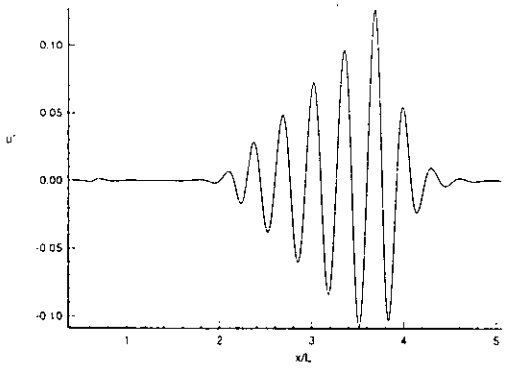


Figure 14: The growth of disturbance streamwise velocity at $yRe^{0.5}/L = 0.36$ for the flat plate separation bubble test case. The Reynolds-number is $10^5$ and the reference length $L = 0.05m$. The disturbances are introduced by blowing and suction at the wall upstream of the separation bubble.The mean flow is from the 9% velocity jump case.

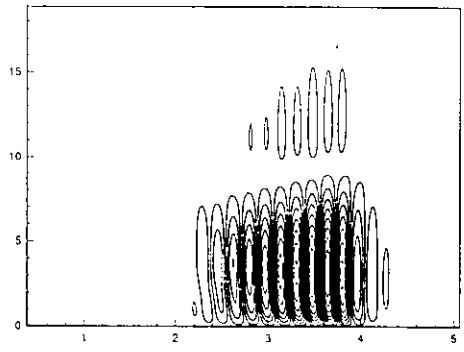


Figure 15: Disturbance streamwise velocity contours for the flat plate separation bubble test case. The Reynolds-number is $10^5$ and the reference length $L = 0.05m$. The disturbances are introduced by blowing and suction at the wall upstream of the separation bubble.The mean flow is from the 9% velocity jump case.